

A 1 Mbps 158 pJ/bit Bluetooth Low Energy (BLE) Compatible Backscatter Communication Uplink for Wireless Neural Recording in an Animal Cage Environment

James Rosenthal¹, Alexandra Pike² and Matthew S. Reynolds¹

¹Dept. of Electrical & Computer Engineering, University of Washington, Seattle, WA, USA

² Juanita High School, Kirkland, WA, USA

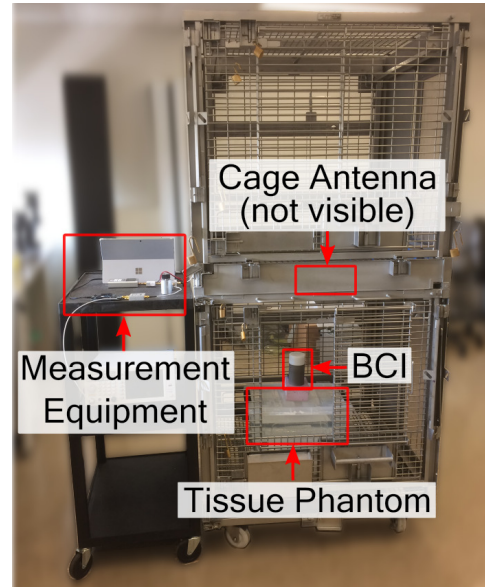
Abstract—Neuroscience research in non-human primates (NHPs) would benefit from multi-day neural recordings from freely moving animals in unconstrained home cage environments. However, wireless brain-computer interfaces (BCI) face two major challenges. First, a metal animal cage forms a reverberant cavity that leads to dense multipath, impairing the wireless communication channel. Second, the battery life of existing wireless neural recording devices is limited by the energy consumption of the neural data uplink.

In this paper, we characterize the channel transfer function of a metal NHP home cage in the 2.4 GHz industrial, scientific, and medical (ISM) band, and demonstrate that there is adequate signal strength and bandwidth to support low-power Bluetooth Low Energy (BLE) compatible backscatter data uplinks. For a typical cage and antenna system, the measured maximum insertion loss of the cage-antenna system was 27.4 dB and the minimum -3 dB bandwidth was 5.0 MHz. We demonstrate a 1 Mbps BLE compatible backscatter communication link achieving a worst-case packet error rate of 1.05%, yielding an effective bit error rate of 5.6×10^{-5} , exceeding the BLE requirement of $\leq 10^{-3}$. The backscatter link has a measured energy consumption of 158 pJ/bit, compared with ≈ 10 nJ/bit for existing WiFi and Bluetooth chipsets.

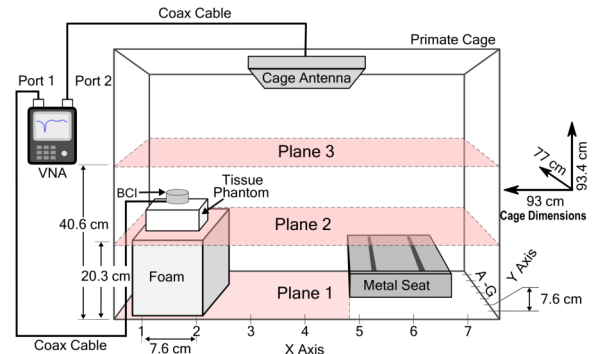
I. INTRODUCTION

In vivo recordings of neural ensemble activity in non-human primates (NHPs) have contributed to the understanding of how neural activity relates to motor function and intent. Traditionally, neural recording has been conducted in constrained environments, such as head-fixed experiments using bulky wired equipment (e.g. rack-mount amplifiers) to achieve high data throughput and reduce measurement noise. However, these setups result in unnaturally stereotyped data [1] and reduced experimental time [2]. As a result, there has been a strong demand in the neuroscience research community for wireless brain-computer interfaces (BCIs) that could measure neural activity in freely moving animals over long durations (>2 days) in unconstrained environments [2]–[4].

The high energy consumption of conventional wireless uplinks results in impractically large batteries given the long operating duration (e.g. days or weeks) desired by neuroscience researchers. Commercial wireless standards such as WiFi and Bluetooth Low Energy (BLE) have per-bit energy consumption between 4-10 nJ/bit, reducing effective battery life [5]. In contrast, backscatter communication uplinks sepa-



(a)



(b)

Fig. 1: (a) Photo and (b) Block diagram of the test setup used to characterize the 2.4 GHz ISM-band wireless channel inside the NHP cage

rate the functions of modulation and carrier generation. In a backscatter uplink, the power and complexity burden of radio frequency carrier wave (RF CW) synthesis is pushed from an energy-poor sensor (such as a neural recording device) to an energy-rich external system (such as a cage-mounted reader). The external system emits the RF CW, and the backscatter-

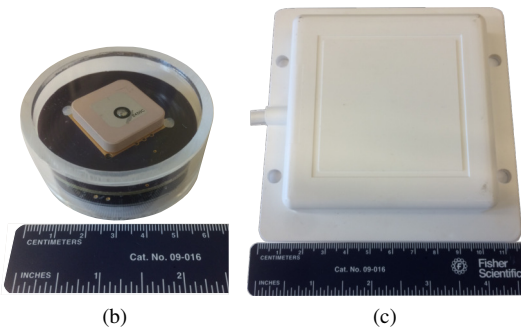
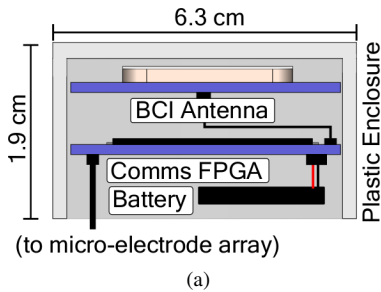


Fig. 2: (a) Drawing (b) Photo of the NeuroDisc BCI (c) Photo of the commercial off the shelf (COTS) cage antenna

based device then modulates the impedance presented to its antenna to selectively reflect the incident CW back to the external system. This process enables the backscatter-based device to generate ASK, FSK, PSK, or QAM signals [6], [7].

Two constraints have limited the use of backscatter uplinks in prior neural recording devices. The first constraint is that backscatter uplinks require round-trip paths, making them significantly more susceptible to multipath fading, such as in the reverberant cavity environment of a metal animal cage [8]. The second constraint is that backscatter uplinks have traditionally required custom receiver (reader) solutions, making them difficult to integrate into existing research infrastructure. While recent work has developed backscatter systems that are compatible with standard protocols, such as BLE [5] and WiFi (IEEE 802.11) [9], none have yet explored whether such compatible backscatter systems could successfully uplink biotelemetry from inside a metal animal cage.

To address these constraints, we present a backscatter uplink operating in the 2.4 GHz industrial, scientific, and medical (ISM) band that is compatible with unmodified BLE receivers (e.g. smartphones, tablets, PCs). This uplink has an analog communication energy efficiency of 158 pJ/bit, and can operate with <1% packet error rate (PER) inside a reverberant metal cage environment. This research expands upon prior work in backscatter neural telemetry [8], [10]. This paper also extends prior work in the performance of RFID backscatter links in reverberation chambers [11], [12]. To the authors' knowledge, it presents the first investigation of channel transfer functions (CTFs) inside an NHP cage within the 2.4 GHz ISM band and the first demonstration of a BLE compatible backscatter system operating in a cage environment.

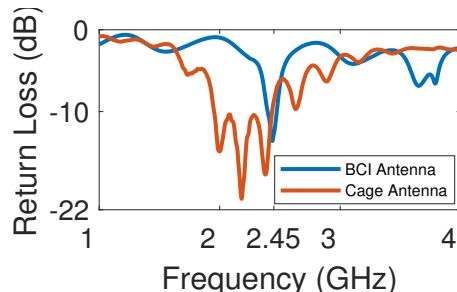


Fig. 3: Measured return loss of the BCI antenna and the cage antenna, outside of the cage environment.

II. 2.4 GHz CHANNEL TRANSFER FUNCTION MEASUREMENT IN AN NHP CAGE

Measurements were conducted in the lower chamber of a standard double-height NHP cage (Fig. 1) having external dimensions of 93.4 cm \times 93 cm \times 77 cm (height \times width \times length). All six cage sides are made of a square metal mesh with a mean gap of 2.5 cm. A 60.7 cm \times 23.4 cm polycarbonate window is inset into one cage wall, and inside the cage there is an 18 cm \times 15 cm metal seat for the NHP.

In our experiments, we used the NeuroDisc BCI which consists of a 2.4 GHz BCI antenna, backscatter modulator, communications FPGA, and battery within a plastic housing (Fig. 2a). The BCI antenna was a semi-custom design consisting of a circular, 5.5 cm diameter, two-layer FR-4 PCB with 1.6 mm dielectric thickness and 30 μ copper trace thickness. The top side of the BCI antenna PCB contained a centered, circularly shaped ground plane and a Tagolas Inc. WLP.2450 ceramic patch element with dimensions 2.5 cm \times 2.5 cm \times 0.4 cm. The bottom side of the PCB contained a balun transformer and a UMC coaxial connector. The measured return loss of this antenna is plotted in Fig. 3. The BCI antenna was connected to port 1 of a Keysight FieldFox Vector Network Analyzer (VNA) with a coaxial cable and placed on top of a tissue phantom inside the cage. The tissue phantom consisted of a 41.8 cm \times 27.8 cm \times 16.5 cm plastic container filled with 7 L of tissue-equivalent saline solution (0.91 g NaCl per liter of distilled water) to approximate the body of an average juvenile male rhesus macaque.

The cage antenna was affixed on the inside of the mesh wall separating upper and lower chambers of the NHP, as shown in Fig. 1. An L-Com Inc. 2.4 GHz 8 dBi right-hand circularly polarized (RHCP) patch antenna (Fig. 2c) selected for the cage antenna was connected to port 2 of the VNA. Circular polarization was employed to reduce polarization mismatch since an NHP may position itself in any orientation relative to the cage antenna. The cage antenna has overall dimensions of 2.3 cm \times 11.6 cm \times 11.6 cm.

Measurements were made at a total of 126 total locations across 3 measurement planes: 28 locations on Plane 1, 49 locations on Plane 2, and 49 locations on Plane 3. The grid spacing was 7.6 cm, with the x-axis labelled A through G and the y-axis labelled 1-7. The vertical spacing was 20.3 cm, labelled Measurement Plane 1, Plane 2, and Plane 3. Columns

TABLE I: CTF measurements summary

	Measurement Plane		
	Plane 1	Plane 2	Plane 3
Minimum Usable BW (MHz)	12.1	5.0	8.1
Mean Usable BW (MHz)	33.3	30.6	28.7
Maximum Insertion Loss (dB)	26.0	27.4	27.4
Mean Insertion Loss (dB)	19.4	17.0	8.8

5-7 on the bottom measurement plane (Plane 1) were unusable due to the NHP bench height. A 2-port VNA calibration, including all cables, was performed to move the reference plane to the antenna ports. The cables were dressed to the cage walls to minimize their influence on the measurements.

A. Experimental Results

The measured insertion loss and “usable bandwidth” (3 dB bandwidth) are presented in the heatmaps and histograms of Figs. 5, 6, and 7, as summarized in Table I. The widest usable bandwidths and best case insertion loss occurred on Measurement Plane 3, and positions near the middle of the cage tended to have wider usable bandwidths and lower maximum insertion losses compared to positions at the edges of the cage. The minimum usable bandwidth across all 126 locations was 5.0 MHz, with means of 33 MHz, 30.6 MHz, and 28.7 MHz on Measurement Plane 1, 2, and 3, respectively. The maximum insertion loss across all 126 locations was 27.4 dB, with means of 19.4 dB, 17.0 dB, and 8.8 dB on Measurement Plane 1, 2, and 3, respectively.

B. Discussion of CTF Measurements

The insertion loss and usable bandwidth data reveal a dense multipath environment inside the NHP cage. The results show that the widest bandwidth and minimum insertion losses occurred in the area directly underneath the receiving antenna, with the narrowest bandwidths and maximum losses near the outside corners. These measurements in the 2.4 GHz ISM band show slightly improved channels compared to measurements previously taken in the same NHP cage in the 915 MHz ISM band [8]. These measurements suggest that it is essential for system designers to consider the deep nulls that result when designing a communication system to operate inside of the cavity formed by an animal cage. For this work we chose to use BLE advertising packets that use 1 MHz bandwidth communication channels with frequency diversity provided by the three distinct advertising channels. In the case of BLE uplinks, deep nulls due to multipath interference can be mitigated by leveraging the frequency diversity between the three advertising channels prescribed by the BLE standard and/or dynamically changing the center frequency of the external carrier wave and the relative subcarrier frequency deviations. For other communication standards, channel equalization techniques could be employed at the cost of greater complexity and higher overall system power consumption.

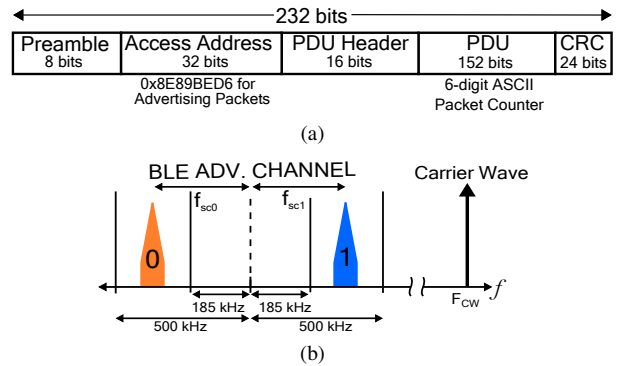


Fig. 4: (a) Overview of the BLE advertising packet structure with the custom packet counter (b) Placement of FSK signal within a BLE advertising channel

III. COMMUNICATION SYSTEM TESTING

A. BLE Advertising Requirements

The BLE standard is well suited for unidirectional backscatter uplinks because the BLE protocol supports an “Advertising” mode where devices broadcast data packets without being required to receive. The physical-layer communication protocol is defined in the BLE v4.0 specification and requires that data be transmitted at 1.0 Msymbol/sec on one of three advertising channels (CH37 at 2.402 GHz, CH38 at 2.426 GHz, and CH39 at 2.480 GHz). Data bits are modulated using frequency-shift keying modulation with frequency deviations between 185 kHz to 500 kHz. A binary ‘one’ is sent by shifting the FSK subcarrier above the channel’s center frequency and a binary ‘zero’ by shifting the FSK subcarrier below the channel center, as shown in Fig. 4b. Data is formatted into advertising packets that include a 24-bit cyclic redundancy check (CRC) and channel-dependent data whitening, as specified in the BLE v4.0 specification and shown in the Fig. 4a.

B. BLE Receiver System

A BLE-compatible backscatter communication system was developed based on work presented in [10]. A Nordic Semiconductor nRF51822 Development Kit (DK) was used as the receiver. The nRF51822 is a commercially-available integrated system-on-chip for BLE applications. An SMA connector was soldered onto the nRF51822 DK to connect the cage antenna to the device; no other modifications were made to the hardware or firmware. The nRF51822 DK was programmed with Nordic Semiconductor’s “nRF sniffer” BLE development firmware that allows the device to transfer data packets via USB to a PC running Wireshark, an open-source packet analyzer software package. Received BLE packets were then parsed and analyzed using Matlab 2018a software (MathWorks, Inc.). All hardware and software used for the receiver could be implemented using a commodity BLE receivers (e.g. smartphones, tablets, laptops) and open-source software platforms (e.g. Android SDK). No hardware or firmware modifications are required because the backscatter signals are fully BLE compatible.

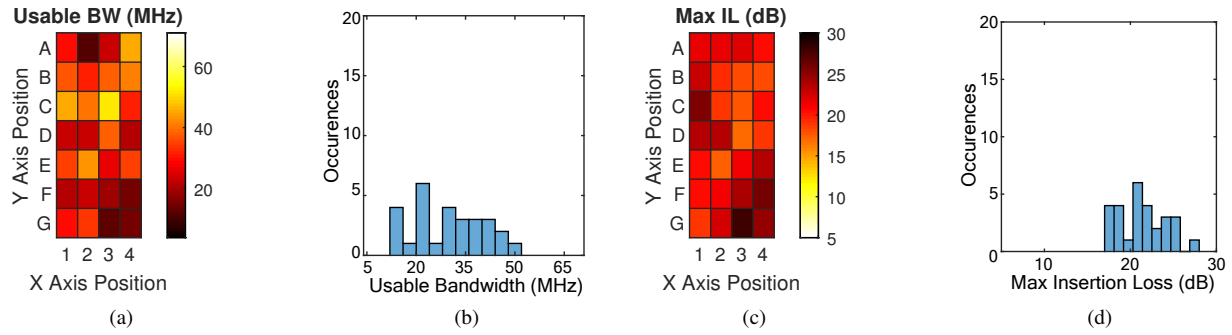


Fig. 5: Experimental results at Measurement Plane 1 showing (a) Heatmap and (b) Histogram of usable bandwidth, (c) Heatmap and (D) Histogram of maximum insertion loss. In all heatmap images, darker colors indicate worse performance.

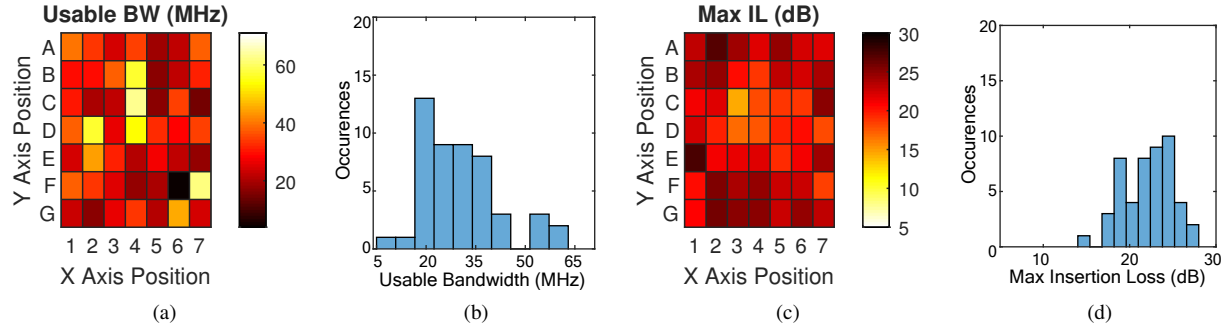


Fig. 6: Experimental results at Measurement Plane 2 showing (a) Heatmap and (b) Histogram of usable bandwidth, (c) Heatmap and (D) Histogram of maximum insertion loss. In all heatmap images, darker colors indicate worse performance.

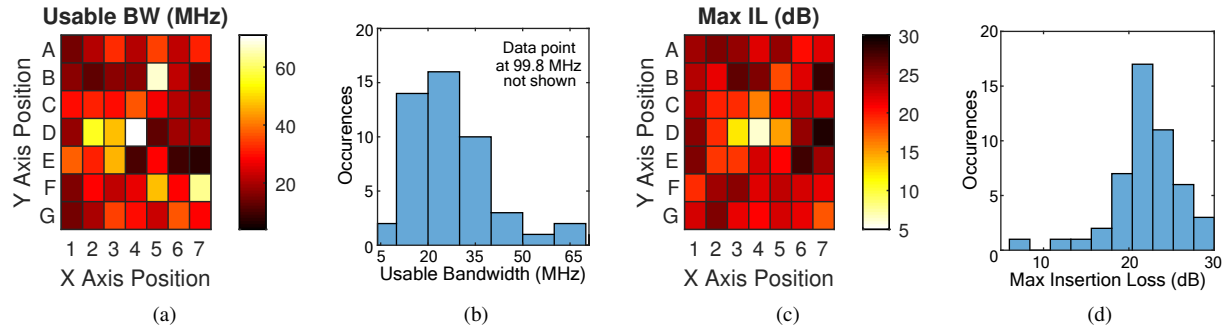


Fig. 7: Experimental results at Measurement Plane 3 showing (a) Heatmap and (b) Histogram of usable bandwidth, (c) Heatmap and (d) Histogram of maximum insertion loss. In all heatmap images, darker colors indicate worse performance.

C. Experimental Setup

A bistatic BLE backscatter system was set up around the NHP cage to evaluate the backscatter uplink performance, as shown in Fig. 8. A carrier wave (CW) source antenna and a BLE receiver (BLE RX) antenna were mounted to the center of the top of the cage, separated by 41 cm. Identical L-Com 2.4 GHz 8 dBi RHCP antennas were used for both the CW source and the BLE RX. The CW antenna was connected to an RF Explorer signal generator (Seed Studio Co. Ltd.) and a PE1516 amplifier (Pasternack Enterprises, Inc.) that supplied a total CW power of +15 dBm. The NeuroDisc BCI with a BLE-compatible backscatter uplink FPGA code was then moved to various measurement locations within the cage. The NeuroDisc device was configured to transmit a packet counter

on each of the three advertising channels allocated by the BLE 4.0 specification. Packet error rate (PER) was then estimated by dividing the number of dropped packets by the total number of packets transmitted, as indicated by the packet counter (Fig. 4a). A minimum of 5800 packets were collected for each test, providing more than 1.34×10^6 bits per measurement location. Any packet that failed a CRC check was marked as a packet error.

To evaluate the PER performance, five points were chosen on each measurement plane, and PER was measured on each of the three BLE advertising channels, for 45 total measurements. Due to the metal seat inside the cage, PER measurements were made at locations B2, F2, B4, D4, and F4 for Measurement Plane 1 while PER measurements were made at locations B2,

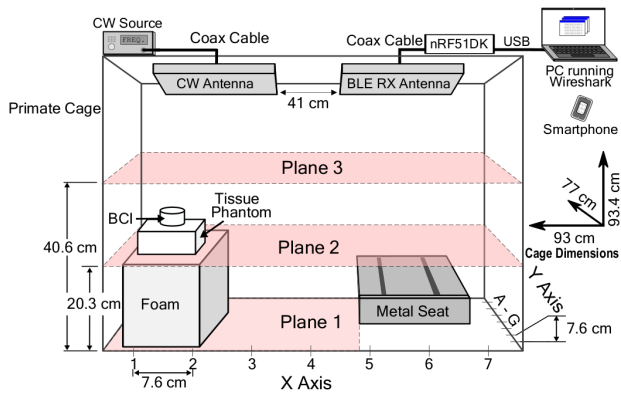


Fig. 8: Block diagram of the test setup used to characterize the wireless BLE backscatter uplink inside the NHP cage

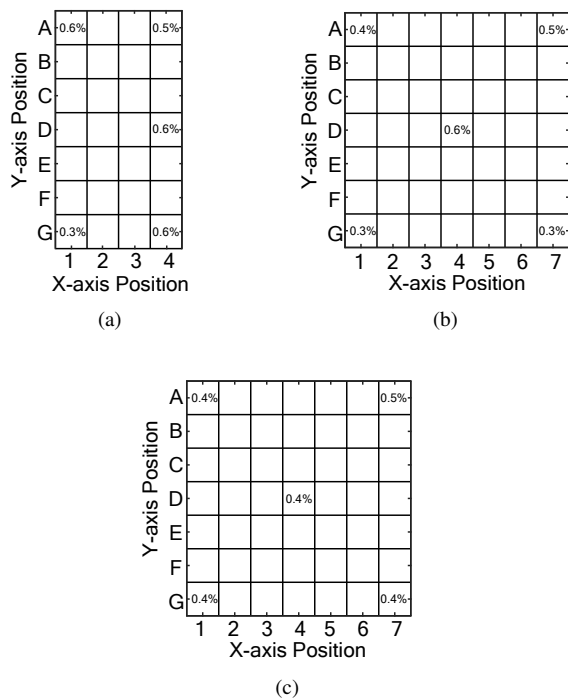


Fig. 9: Mean BLE packet error rate (PER) measurements across all three channels for (a) Measurement Plane 1, (b) Plane 2, and (c) Plane 3 inside the NHP cage. At each measurement location, ≥ 5800 packets were transmitted, corresponding to a minimum of 1.35×10^6 bits. Measurements from all planes indicate a worst-case PER of $< 1.3\%$.

F2, D4, B6, and F6 for Measurement Planes 2 and 3 (Fig. 8).

D. Experimental Results

The PER performance of the BLE-compatible backscatter uplink is summarized in Fig. 9 and in Table II. We found Channel 39 to have the lowest PER across all testing locations; Channels 38 and 39 had less than 1% PER across all testing locations, ranging from a best case of 0.27% to a worst case of 0.92% with a mean PER of 0.58%. Channel 37 had the highest PER with a best case of 0.46%, a worst case of 1.29%, and mean of 0.80%.

TABLE II: Summary of the packet error rate (PER) measurements

	Measurement Plane		
	Plane 1	Plane 2	Plane 3
Best-Case PER	0.32% (CH39)	0.27% (CH39)	0.33% (CH39)
Worst-Case PER	1.29% (CH37)	1.03% (CH37)	1.05% (CH37)
Mean PER	0.69%	0.60%	0.69%

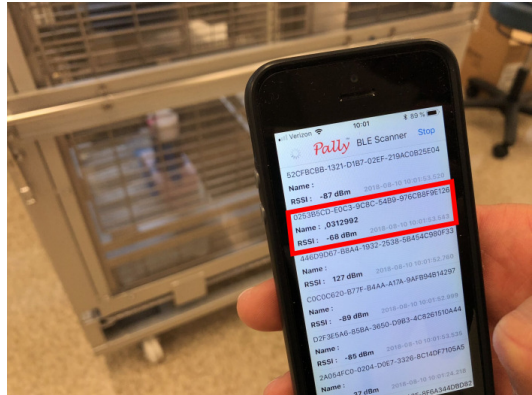


Fig. 10: Backscattered BLE advertising packets received by an unmodified smartphone outside of the cage

Across all three advertising channels, the best- to worst-case PERs were 0.32% to 1.29%, 0.27% to 1.03%, and 0.33% to 1.05% for Measurement Planes 1, 2, and 3 respectively. Mean PERs were 0.69%, 0.60%, and 0.69% for Planes 1, 2, and 3 respectively. The NHP cage appeared to function as a chaotic cavity with no obvious pattern to where the best- and worst-case scenarios occurred. Additionally, because the wire mesh cage did not form a complete Faraday cage, we observed that an unmodified smartphone could receive the backscattered packets from outside the cage at a distance of 2-3 meters, as shown in Fig. 10.

E. Discussion of PER Measurements

A PER of $< 1.3\%$ across all measurement locations and all channels inside the cage demonstrate the viability of using ultra-low power BLE-compatible backscatter to uplink biotelemetry from freely moving animals in an unconstrained cage environment. If we assume that each packet error results from a single bit error, and that each error is independent, we can calculate the effective bit-error rate (BER) as

$$\text{BER} = 1 - (1 - \text{PER})^{\frac{1}{n}}, \quad (1)$$

where n is the number of bits per packet, in this case 232. From Eq. 1 we find the worst-case measured PER yields an effective BER of 5.6×10^{-5} which meets the BLE v4.0 specification requirement of $\text{BER} \leq 10^{-3}$.

IV. CONCLUSION & FUTURE WORK

In this work we provide measurements of the 2.4 GHz channel transfer function inside the reverberant cavity environment of a metal NHP home cage. Measurements taken in 3 measurement planes using a calibrated VNA indicate a mean

insertion loss of 15.1 dB and a mean usable bandwidth of 30.9 MHz, suggesting that there is a larger usable bandwidth and less insertion loss at the 2.4 GHz ISM band inside of the cage than at the 915 MHz ISM band, as reported in [8].

We then loaded a BLE-compatible backscatter configuration into the FPGA on the NeuroDisc brain-computer interface (BCI). The resulting backscatter-based BLE data uplink consumed only 158 pJ/bit while achieving a worst-case BER of 5.6×10^{-5} . We additionally demonstrated that an unmodified smartphone can receive BLE packets from outside the cage. These results suggest that BLE-compatible backscatter uplinks are a viable solution for telemetering wireless neural data in a research animal cage environment.

Future work will focus on maturing the BLE backscatter uplink for *in vivo* experiments on freely moving NHPs. Algorithms will be developed for the NeuroDisc BCI to send biological data such as neural spike counts within BLE advertising packets. A user interface will be developed to support near real-time analysis of BLE packets on smartphones, tablets, and PCs. Additionally, the BLE backscatter uplink could be integrated with a high-rate custom backscatter uplink to provide redundant and/or complementary wireless uplinks during neuroscience experiments.

ACKNOWLEDGMENT

This material is based upon work supported by the National Science Foundation Graduate Research Fellowship under Grant No. DE-1762114, and in part by Award Number EEC-1028725 from the National Science Foundation. The content is solely the responsibility of the authors and does not necessarily represent the official views of the National Science Foundation. The authors would also like to thank Prof. Azadeh Yazdan-Shahmorad and the team at the Washington National Primate Research Center for providing access to the NHP cage.

REFERENCES

- [1] A. Jackson, J. Mavoori, and E. E. Fetz, "Correlations between the same motor cortex cells and arm muscles during a trained task, free behavior, and natural sleep in the Macaque monkey," *Physiology*, vol. 97, no. 1, pp. 360–374, Jan. 2007.
- [2] S. Zanos, A. G. Richardson, L. Shupe, F. P. Miles, and E. E. Fetz, "The Neurochip-2: an autonomous head-fixed computer for recording and stimulating in freely behaving monkeys," *IEEE Trans. Neural Syst. Rehabil. Eng.*, vol. 19, no. 4, pp. 427–435, 2011.
- [3] M. Yin *et al.*, "Wireless neurosensor for full-spectrum electrophysiology recordings during free behavior," *Neuron*, vol. 84, no. 6, pp. 1170 – 1182, 2014.
- [4] J. Rosenthal, E. Kampianakis, A. Sharma, and M. Reynolds, "A 6.25 Mbps, 12.4 pJ/bit DQPSK backscatter wireless uplink for the NeuroDisc brain-computer interface," in *Biomedical Circuits and Systems Conference (BioCAS), 2018 IEEE*, Oct 2018.
- [5] J. F. Ensworth and M. S. Reynolds, "Every smart phone is a backscatter reader: Modulated backscatter compatibility with Bluetooth 4.0 Low Energy (BLE) devices," in *Proc. 2015 IEEE Intl. Conf. RFID*, 2015.
- [6] J. Kimionis, A. Bletsas, and J. N. Sahalos, "Increased range bistatic scatter radio," *IEEE Transactions on Communications*, vol. 62, no. 3, pp. 1091–1104, March 2014.
- [7] S. J. Thomas and M. S. Reynolds, "A 96 Mbit/sec, 15.5 pJ/bit 16-QAM modulator for UHF backscatter communication," in *Proc. IEEE Intl. Conf. RFID (RFID 12)*, Apr. 2012, pp. 185–190.
- [8] E. Kampianakis, A. Sharma, J. Rosenthal, and M. S. Reynolds, "Wide-band UHF DQPSK backscatter communication in reverberant cavity animal cage environments," *IEEE Trans. on Antennas and Propagation (TAP)*, (to appear) 2019.
- [9] B. Kellogg, V. Talla, S. Gollakota, and J. R. Smith, "Passive Wi-Fi: Bringing low power to Wi-Fi transmissions," in *Proc. 2016 Usenix Conf. on Networked Systems Design and Implementation*. Berkeley, CA, USA: USENIX Association, 2016, pp. 151–164.
- [10] J. Rosenthal and M. S. Reynolds, "A 158 pJ/bit 1.0 Mbps Bluetooth Low Energy (BLE) compatible backscatter communication system for wireless sensing," in *Proc. IEEE Topical Conference on Wireless Sensors and Sensor Networks (WiSNet)*, Jan. 2019.
- [11] J. H. Rudander, I. e Khuda, P. Kildal, and C. Orlenius, "Measurements of RFID tag sensitivity in reverberation chamber," *IEEE Antennas and Wireless Propagation Letters*, vol. 10, pp. 1345–1348, 2011.
- [12] L. Kon, R. Kassi, and N. Rolland, "UHF RFID tags backscattered power measurement in reverberation chamber," *Electronics Letters*, vol. 51, no. 13, pp. 972–973, 2015.